

# Visualizing RNA splicing *in vivo*

Gayatri Gowrishankar and Jianghong Rao\*

DOI: 10.1039/b617574k

Ribozymes are RNA molecules capable of associating with other RNA molecules through base-pairing and catalyzing various reactions involving phosphate group transfer. Of particular interest to us is the well known ribozyme from *Tetrahymena thermophila* capable of catalyzing RNA splicing in eukaryotic systems, chiefly because of its potential use as a gene therapy agent. In this article we review the progress made towards visualizing the RNA splicing mediated by the *Tetrahymena* ribozyme in single living mammalian cells with the  $\beta$ -lactamase reporter system and highlight the development made in imaging RNA splicing with the luciferase reporter system in living animals.

## Introduction

As per the 'central dogma' of molecular biology, RNA molecules occupy the second stage in the process of information transfer from the genetic blueprints in the DNA molecules to the molecular motors—the proteins. In 1982, however, Tom Cech made the completely unexpected discovery that RNA from a unicellular protozoan called *Tetrahymena thermophila* could perform auto-splicing.<sup>1</sup> This discovery jump-started widespread research into the structure, function, and mechanism of

action of ribozymes or RNA enzymes. The *Tetrahymena* ribozyme, which will be the focus of this article, has been instrumental in helping the scientific world understand ribozymes and the mechanics of *cis* and *trans*-RNA splicing.

## The *Tetrahymena* ribozyme

Self-splicing by the group I intron of the *Tetrahymena* rRNA involves two *trans*-esterification reactions (Fig. 1). The intron recognizes the splice sites through an intron-encoded sequence called the internal guide sequence, or IGS. The 5' and 3' exons are thought to align on the IGS and form a pseudoknot structure consisting of two stems (P1 and P10). The first step is initiated by guanosine or one of its 5'-phosphorylated forms which attacks the phosphorous atom at the 5'-splice site and forms a

3',5'-phosphodiester bond to the first nucleotide of the intron. The 5' exon, now terminating in a free 3'-hydroxyl group, then attacks the phosphorous atom at the 3'-splice site. Completion of the two-step reaction results in ligation of the exons and excision of the intron.<sup>2</sup>

Deleting the first 21 nucleotides of the group I intron afforded a derivative known as L-21, which was shown to mediate *trans*-splicing (between two separate RNA molecules) *in vitro*,<sup>3,4</sup> in *E. coli*<sup>5</sup> and in mammalian cells.<sup>6</sup> The IGS of the ribozyme may be modified to base-pair essentially with any sequence as long as a G–U wobble pair is maintained at the splice site. Because of this sequence latitude, ribozymes based on the group I intron of *Tetrahymena* can be engineered to target any chosen RNA. Sequences present downstream of the ribozyme are ligated to the splice site of the substrate

*Molecular Imaging Program at Stanford, Department of Radiology & Bio-X Program, Cancer Biology Program, Stanford University School of Medicine, 1201 Welch Road, Stanford, California 94305-5484, USA. E-mail: jrao@stanford.edu; Fax: (+1) 650-736-7925*



Gayatri Gowrishankar

*Dr Gayatri Gowrishankar is a postdoctoral scholar working in the Molecular Imaging Program in the Radiology Department at Stanford University School of Medicine. She received her PhD in Biochemistry from the University of Hannover, Germany in Biochemistry, where she trained in the Medical School as an RNA biologist. She is currently focusing on evolving an mRNA imaging strategy using the Tetrahymena ribozymes.*



Jianghong Rao

*pharmacology at the University of California, Los Angeles, as an assistant professor after two years of postdoctoral training in the laboratory of Professor Roger Y. Tsien at the University of California, San Diego. He received his BS in chemistry from Peking University, China, and a PhD from the department of chemistry and chemical biology at Harvard University under the guidance of Professor George M. Whitesides. His current research includes the develop-*

*ment of novel molecular probes and imaging strategies for in vivo imaging of gene expression and for early disease detection and diagnostics.*

*Dr Jianghong Rao is Assistant Professor of Radiology and a member of the Molecular Imaging Program at Stanford University. Previously, he was in the department of molecular and medical*

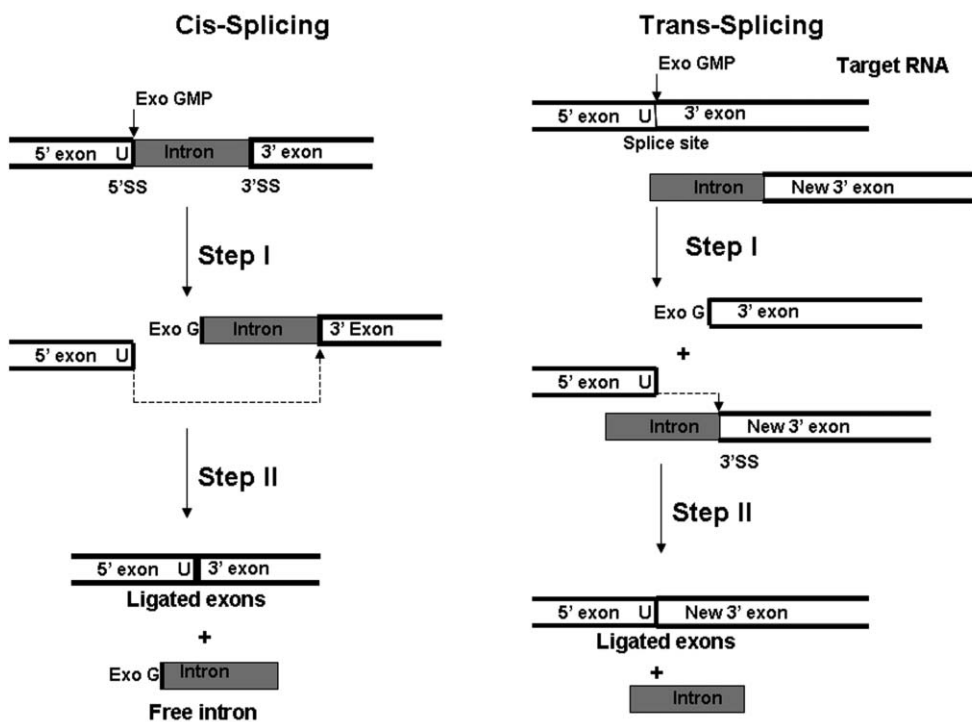


**Fig. 1** Schematic of the two-step group I intron splicing. (A) *cis*-Splicing of the intron from a single precursor RNA resulting in a ligated exon and excised intron. (B) *trans*-Splicing between a 5' exon (target RNA) and a new 3' exon located on a separate RNA, directed by the internal guide sequence (IGS) of the ribozyme (not shown here). Splicing occurs at uridine (U) in the target RNA, which forms a wobble base pair with a guanine in the IGS.

RNA. These 3' exon sequences may also be changed to potentially any nucleotide sequence. This ability was thus used to 'revise' mutant RNA in a new gene therapy approach termed ribozyme-mediated RNA repair.

Compared with more traditional strategies, RNA repair would allow the endogenous regulation of the gene modification (as it is RNA directed) and simultaneously reduce the expression of the mutant gene product. This approach has been successfully used to correct sickle cell transcripts,<sup>7</sup> to remedy the triplet repeat expansion in the 3' UTR of the myotonic dystrophy protein kinase transcript,<sup>8</sup> to repair mutant p53 transcripts<sup>9</sup> and the mutant mRNA of canine skeletal muscle chloride channel,<sup>10</sup> and to convert pathogenic transcripts of the hepatitis C virus (HCV) into new RNAs that exert anti-HCV activity.<sup>11</sup> These ribozymes have also been used to *trans*-splice a cytotoxic gene onto a particular target RNA,<sup>12,13</sup> ensuring a target-specific expression of the cytotoxic gene. Kwon *et al.* used this approach to kill cancer cells overexpressing the human telomerase reverse transcriptase

(hTERT) RNA. Whereas cleaving ribozymes must efficiently deplete a chosen mRNA species to be effective *in vivo*, even a small amount of *trans*-splicing would be sufficient to express the cytotoxic gene and kill the target gene-expressing cells.

### Need for imaging splicing *in vivo*

Much about the splicing reaction has been learned from extensive *in vitro* biochemical and structural studies; however, these studies do not fully reflect the characteristics of splicing *in vivo*, which is critical to the therapeutic application of ribozymes. While *in vitro trans*-splicing occurred with a half-life of 13 min, converting 85–90% of precursor RNA to product RNA,<sup>5</sup> the reaction was observed to splice only 25–50% of targeted transcripts *in vivo*.<sup>6</sup> Moreover, it has been reported that the splicing product may not be translated efficiently in mammalian cells.<sup>14</sup> This low efficiency is blamed on the complex intracellular environment of mammalian cells. It has also been found that the exon context

surrounding the ribozyme sequence greatly affects its folding, and hence its catalytic activity.<sup>15</sup> Since the *Tetrahymena* ribozyme would be used as a gene therapy agent in mammalian cells, there arose a need to directly assay ribozyme activity *in vivo*. The *in vivo* assay could be subsequently applied to discover ribozyme variants that can function better in the mammalian cellular environment.

The first *in vivo* demonstration of *Tetrahymena* self-splicing was realized in *Escherichia coli* in the 1980's. The *Tetrahymena* intron was inserted into the  $\beta$ -galactosidase gene, such that the expression of the reporter was dependant on the self-splicing by the ribozyme<sup>16,17</sup> and used to phenotypically assess the effect of mutations in key nucleotides. Thus the utility of detecting the ribozyme activity by linking the ribozyme to well-known reporter systems was understood even back then. Similarly the firefly luciferase gene and luciferase activity were used to demonstrate self-splicing in mammalian cells.<sup>14</sup> But these methods lacked single-cell resolution or required cell permeabilization which greatly

reduced survival rates. Following the more recent advances in molecular imaging techniques, imaging probes and instrumentation, it has become possible to visualize both *cis*- and *trans*-splicing events in single living cells and in living animals.<sup>18,19</sup>

## Imaging the ribozyme self-splicing in live mammalian cells

To visualize the self-splicing ribozyme in live mammalian cells, we utilized a new reporter enzyme, TEM-1  $\beta$ -lactamase (Bla), a small (29 kDa), monomeric bacterial enzyme. With the development of several fluorogenic substrates including CCF2/AM and CC1, Bla has become a sensitive and versatile reporter system for detecting or imaging biological processes and interactions in mammalian cells.<sup>20,21</sup> We developed constructs in which the self-splicing *Tetrahymena thermophila* group I intron ribozyme was inserted into the ORF of the mRNA of Bla (Fig. 2A).<sup>18</sup> These constructs were driven by a CMV promoter for expression in mammalian cells. CCF2/AM was used to visualize the ribozyme-dependant Bla activity in single living cells. A scheme explaining how CCF2 works is shown in Fig. 2B. Briefly if the cells do not express Bla, CCF2 fluoresces green under violet excitation owing to

intramolecular fluorescence resonance energy transfer (FRET) between the coumarin donor and the fluorescein acceptor. In the presence of Bla, CCF2 is hydrolyzed, resulting in the spontaneous elimination of the fluorescein acceptor and a dramatic increase in the blue coumarin fluorescence as a result of loss of FRET. Thus the ratio of blue to green fluorescence for an individual CCF2/AM treated cell is dependant on the activity of the ribozyme.

COS 1 or COS 7 cells were transfected with the specific ribozyme constructs, loaded with CCF2/AM and incubated for 1 h. The stained cells were examined either by fluorescence microscopy (Fig. 3A–C) or flow cytometry (Fig. 3E) to assess ribozyme activity with a single cell resolution. A red fluorescent protein—DsRed was used as a transfection marker to normalize the observed ribozyme activity for variations in transfection efficiency.

The compatibility of this reporter system with flow cytometry allowed live-cell screening for variants of the ribozyme with the highest splicing efficiency. We analyzed variants that had different insertions (from 4 to 84) in the middle of the L1 loop—the region that is located between the splice site and the IGS (Fig. 3D). COS 7 cells were transfected with these ribozyme constructs and DsRed as a co-transfection marker

and then analyzed by fluorescence-activated cell sorting (FACS). As FACS allowed the isolation of cell populations based on differences in fluorescence emission, we identified a ribozyme variant (RzL + 4) that displayed a 4-fold better Bla activity and displayed substantially more Bla positive cells than the wild-type ribozyme.<sup>18</sup>

This study demonstrated the exciting possibility of using the ribozyme– $\beta$ -lactamase reporter system to screen large combinatorial libraries of ribozymes directly in live mammalian cells and identify improved mutants. This method may facilitate the discovery of ribozyme variants that can function better in the mammalian cellular environment. While this study focused on insertions in the L1-loop, mutations at other sites could be similarly examined. We have generated a library of ribozyme variants using random mutagenesis, and from the FACS screening identified a variant with a single mutation that displayed an improved *cis*-splicing activity—the final Bla activity was 3-fold higher than the wild-type ribozyme reporter.<sup>22</sup>

## Imaging *trans*-splicing in single cells

Although visualizing *cis*-splicing of the *Tetrahymena* ribozyme in mammalian

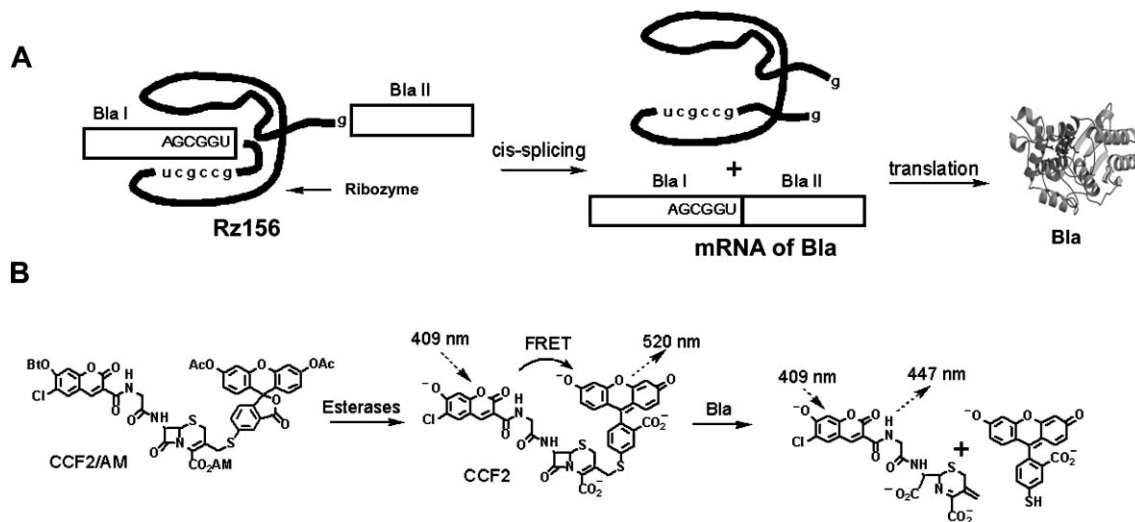


**Fig. 2** The ribozyme–Bla reporter system. (A) Schematic representation of splicing-dependent Bla reporter gene strategy. The ribozyme reporter Rz156 consists of the *Tetrahymena* intron and a broken Bla ORF (BlaI and BlaII). Ribozyme self-splicing produces uninterrupted mRNA of Bla, which is translated into the reporter enzyme Bla. (B) The *in vivo* assay uses CCF2/AM. Membrane-permeable CCF2/AM is converted to CCF2 by intracellular esterases. When no Bla is present, CCF2 fluoresces green (at 520 nm) because of fluorescence resonance energy transfer (FRET) from the coumarin donor to the fluorescein acceptor. Bla hydrolysis splits off the fluorescein, disrupts FRET, and shifts the emission to blue (at 447 nm) (Adapted from ref 18; Copyright 2004 The National Academy of Sciences of the USA).

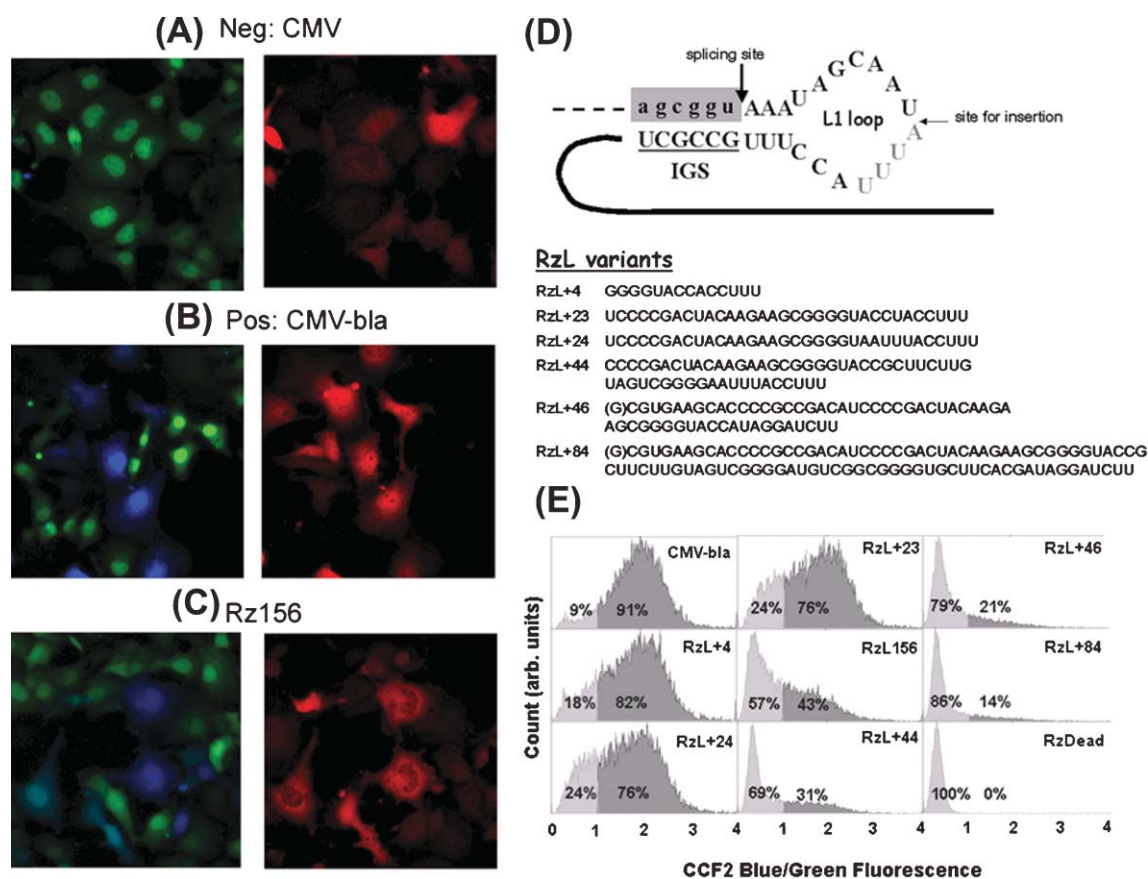


**Fig. 3** Imaging *cis*-splicing *in vivo*. (A–C) Fluorescence microscopy images of the COS 1 cells transfected with an empty vector (CMV) (A) or transiently transfected with CMV-bla (B) or with Rz156 (C). (A–C *Left*) An overlay of frames captured at 530 nm (green emission) and 460 nm (blue emission). (A–C *Right*) DsRed emission at 605 nm with excitation at 560 nm. Nontransfected cells show no Bla activity (green in *Left* and black in *Right*). (D) Ribozyme variants with insertion of nucleotides at the indicated site of the L1 loop of the *Tetrahymena* ribozyme. (E) Fluorescence-activated cell sorter analysis of COS 7 cells transiently transfected with construct CMV-bla (positive control), RzL + 4, RzL + 24, RzL + 23, RzL156, RzL + 44, RzL + 46, RzL + 84, or a ribozyme dead mutant (RzDead, a negative control). DsRed cDNA was cotransfected as a transfection marker. Cells were incubated with CCF2/AM for 1 h before fluorescence-activated cell sorter analysis. The populations depicted consist of cells that were healthy (as judged by forward and side scatter) and DsRed-positive. For easy comparison of different constructs, the percentages of Bla-positive (dark gray area) and Bla-negative (light gray cells (defined as blue–green ratios >1 and <1, respectively) are indicated for each construct (Adapted from ref 18; Copyright 2004 The National Academy of Sciences of the USA).

cells was a significant step forward in the context of establishing a novel screening method for identifying ribozyme variants, it is the *trans*-splicing form of the ribozyme that is of interest to gene therapy proponents. Therefore, two approaches were followed to design a similar mammalian cell-based assay that can be applied to systematic screening for *trans*-splicing ribozyme variants with improved *in vivo* efficiency.

In the first approach we utilized a split  $\beta$ -lactamase reporter system. We constructed a *trans*-splicing ribozyme with one part of the Bla mRNA (Bla II in Fig. 2A) attached to its 3' end. The IGS was modified to recognize the other part of the Bla mRNA (Bla I).<sup>19</sup> It had been previously reported that for *trans*-splicing ribozymes to work effectively it

was essential to add extended flanking sequences at the 3' end of the substrate RNA and the complementary sequence to the 5' end of the *trans*-splicing ribozyme.<sup>9,12</sup> Hence we added a 211 nt sequence derived from the mRNA of DsRed to the 3' end of Bla I and the corresponding antisense sequence to the 5' end of Bla II (Fig. 4A). When expressed together, a *trans*-splicing reaction would take place in mammalian cells and produce the complete, translatable Bla mRNA whose activity can be fluorescently imaged. Fig. 4B and C show that for the first time the *trans*-splicing activity of the *Tetrahymena* ribozymes could indeed be visually detected in single living mammalian cells. For nontransfected COS 7 cells, the blue/green ratio was low (<0.5), and for transfected

cells 51.1% had a high blue/green ratio of >1.0. All cells with high blue/green ratio also emitted red fluorescence from the transfection marker DsRed, supporting the fact that reported Bla activity comes from the *trans*-splicing ribozyme.

This split ribozyme- $\beta$ -lactamase reporter approach was extended to detect *trans*-splicing between a clinically relevant mRNA target and ribozymes in mammalian cells.<sup>23</sup> In this design each half of the reporter was equipped with antisense sequences to a target p53 mutant mRNA. The presence of the target p53 mutant mRNA assembled the two halves of the split reporter, facilitated splicing and generated a complete  $\beta$ -lactamase mRNA. This reporter construct can sense the p53 mutant mRNA in mammalian cells, but the

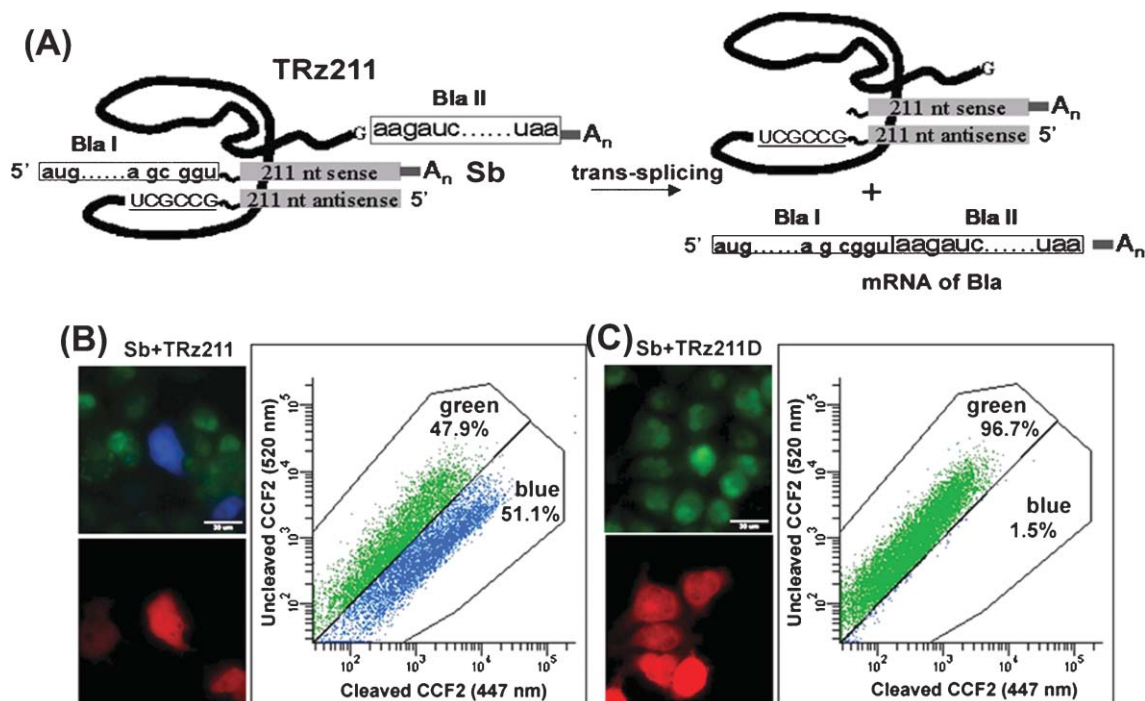


**Fig. 4** Imaging RNA trans-splicing in live cells. (A) Schematic presentation of the strategy for visualizing trans-splicing ribozyme activity by Bla. (B–C) Fluorescence microscopy and FACS analyses of COS 7 cells transiently transfected with (B) Sb (the substrate target RNA) + TRz211 (*trans*-splicing ribozyme), or (C) Sb + TRz211D (catalytically inactive *trans*-splicing ribozyme). DsRed was used a transfection marker in all samples. Each upper image is an overlay of frames captured at 530 nm (green emission) and 460 nm (blue emission); each lower image is DsRed emission at 605 nm excited at 546 nm. Cells with no Bla activity are green in upper images. The scale bar is 30  $\mu$ m. FACS analyses were performed on the DsRed-positive (transfected) cells. The percentages of Bla-positive (blue) and Bla-negative (green) cells (defined as blue–green ratios >1 and <1, respectively) are indicated for each construct. (Adapted from ref 19; Copyright 2004 American Chemical Society).

efficiency of the three-component assembly is currently not high enough to enable single live cell imaging.

The second approach is similar to the traditional *trans*-splicing ribozyme design described in previous papers by Sullenger *et al*<sup>9</sup> (Fig. 5). The new *trans*-splicing ribozyme reporter construct contained three domains—for targeting, splicing and imaging. While the 5' end of the ribozyme has a 200 nt antisense sequence targeting the p53 mutant mRNA, at the 3' end we attached the complete coding sequence of  $\beta$ -lactamase without its start codon. The start codon

AUG of the reporter gene was removed to minimize the reporter translation before the *trans*-splicing. *trans*-Splicing between the ribozyme and the mRNA target would generate a fusion reporter gene that contains the start codon from the target mRNA and becomes translatable. Using this approach, we have successfully imaged over-expressed p53 mutant mRNA in single live mammalian cells.<sup>24</sup>

Both methods could be potentially applied in performing *in vivo* optimization of *trans*-splicing ribozymes. Furthermore, as they are compatible

with the flow cytometry-based screening, they possess a unique advantage over other screening methods in that there is the ability to perform both negative (for minimal background in the absence of a target RNA) and positive selections (for maximal activity in the presence of target RNA).

## Visualizing splicing in live animals

With the rapid advances in molecular imaging techniques, molecular imaging probes are increasingly being used to

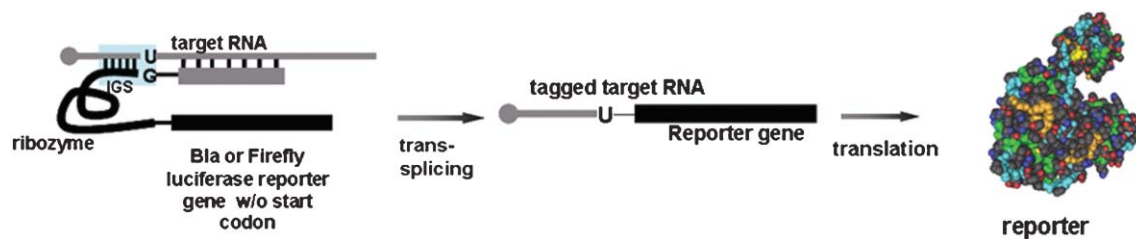


**Fig. 5** Schematic representation of the *trans*-splicing ribozyme mediated detection of a target mRNA. The ribozyme reporter transduces the target mRNA into a fusion reporter mRNA, and subsequent translation of the fusion mRNA produces reporter enzymes that can generate readout signal, for example, fluorescence or bioluminescence emission, for non-invasive *in vivo* imaging.

evaluate the efficacy of drugs or gene therapy agents in preclinical small animal models, thus hastening the translation of these new developments into clinics.<sup>25</sup> While *trans*-splicing ribozymes have been tried and tested in a variety of cell lines, till date few studies have examined the efficacy of these ribozymes in animal models. To visualize ribozyme splicing in animals, a reporter system compatible with small-animal imaging would be needed. We chose to work with the well-established bioluminescent reporter proteins which include different classes of ‘luciferases’. In the presence of molecular oxygen, luciferases react with their substrates ‘luciferin’, resulting in the formation of a luciferase bound peroxyl-luciferin intermediate, which releases photons of visible light<sup>26</sup> that can be detected by sensitive cooled charge-coupled device (CCD) cameras. We replaced the  $\beta$ -lactamase reporter with firefly luciferase and have successfully imaged the splicing of the ribozyme to p53 mutant mRNA in tumor xenografts implanted in living mice.<sup>24</sup> Not only will this be the first time that *Tetrahymena* ribozyme *trans*-splicing has been visualized in living animals but also it will herald a new advancement in the field of RNA imaging. Current strategies using fluorescently or radioactively labeled antisense probes to detect target mRNA by a hybridization mechanism, have met with limited success in living animals.<sup>27–30</sup>

## Visualizing pre-mRNA splicing

In contrast to the ribozyme-mediated visualization of RNA splicing *in vivo*, Bhaumik *et al*<sup>31</sup> developed a different system based on the mammalian spliceosome to image pre-mRNA splicing *in vivo*. The technique, known as spliceosome-mediated RNA *trans*-splicing (SMaRT), was also developed with the intention of repairing disease-causing mutant genes at the level of RNA.<sup>32,33</sup> The principle behind SMaRT is centered on the use of engineered pre-*trans*-splicing molecules (PTMs). Embedded within each PTM are active splicing elements that are recognized by the cell’s splicing machinery and form complexes with the spliceosome and exons that can be *trans*-spliced into the target transcript. The specificity of the *trans*-splicing

reaction is conferred by a binding domain of the PTM which is designed to be complementary to intronic sequences in the target of interest.<sup>34</sup>

Bhaumik *et al* attached a portion of a bioluminescent reporter *Renilla* luciferase<sup>31</sup> as the 3’ exon (Fig. 6A). They designed a target gene that contained the remaining portion of the *Renilla* luciferase coupled with intronic and exonic sequences from the human papilloma virus type 16 (HPV 16). Both RNAs were expressed using a CMV promoter in mouse neuroblastoma cells (N2A). When the PTM *trans*-spliced specifically into the target pre-mRNA, the full length *Renilla* luciferase mRNA and functional protein were produced, generating a bioluminescent signal both *in vitro* and in living mice (Fig. 6B). This study is an excellent example of visualizing pre-mRNA splicing mediated by the mammalian spliceosome *in vivo*.

## Future directions

Hitherto we have visualized the splicing activity of *Tetrahymena* ribozyme through the use of sensitive reporters at the single cell level. An immediate extension of this work is to directly image single ribozyme splicing events in single living cells. There are already reports in which RNA folding and catalysis by the *Tetrahymena* ribozyme was examined at a single molecule level using surface immobilization of dye-labeled ribozymes.<sup>35,36</sup> In recent years great advancements in the field of biological microscopy have allowed cell biologists to track single molecules within single cells.<sup>37</sup> Several techniques have been devised to directly visualize single RNA molecules. These include the use of fluorescently labeled probes for *in vivo* hybridization,<sup>38</sup> caged fluorescent probes and photoactivation,<sup>39</sup> molecular

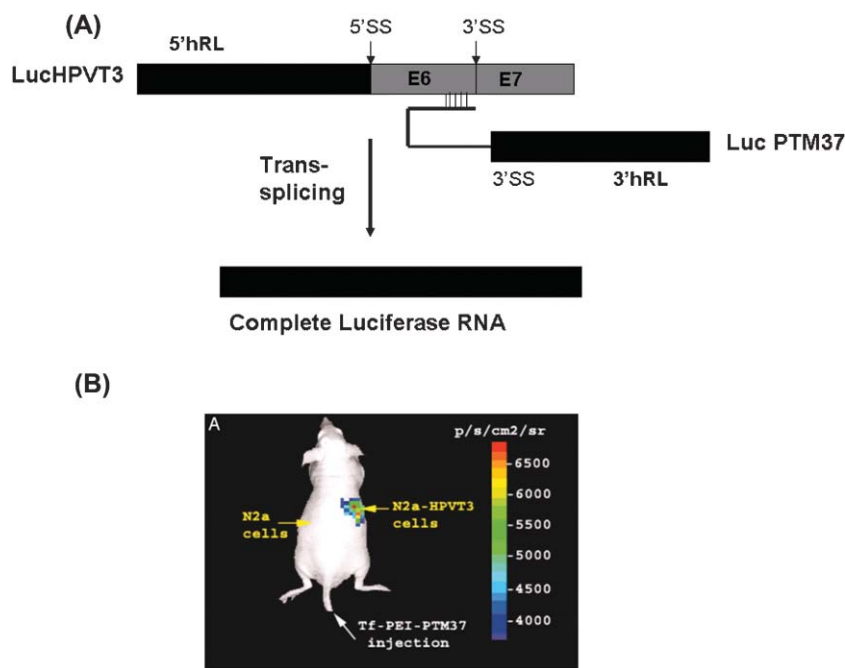


**Fig. 6** Imaging pre-mRNA splicing. (A) Schematic representation of SMaRT reaction. The pre-mRNA target, LucHPVT3, contains the N terminal portion of hRLuc (5’ hRL) coding sequence coupled to exonic and intronic sequences of the HPV-16 E6 and E7 oncoproteins. LucPTM37 codes for the *trans*-splicing components (binding domain, spacer, and 3’ splice elements) as well as the C terminus portion of the hRLuc coding sequence (3’hRL). ss, splice sites. (B) Optical imaging of s.c. tumors in living mice using SMaRT. N2a cells transfected with the pre-mRNA target LucHPVT3, or mock transfected were implanted s.c. onto different sides of a living mouse as shown. Twenty four hours later, the mouse was injected *via* the lateral tail vein with LucPTM37 complexed with transferrin-polyethylene imine (Tf-PEI-PTM37) for delivery to the tumours. 24 h after the delivery the mice were injected with coelenterazine and imaged by using a charge-coupled device camera (Adapted from ref 31; Copyright 2004 The National Academy of Sciences of the USA).

beacons that fluoresce only when the probes have hybridized to the target<sup>40</sup> and the use of a highly specific fluorescent-protein-based labeling system with a single molecule specificity.<sup>41,42</sup> The use of these new probes may be the key to visualizing RNA splicing at a single molecule level in single living cells.

While the strategy of ribozyme-mediated gene therapy is promising, there is still a long way for the current ribozyme to go to the clinics. The establishment and use of a directed *in vivo* evolution process in mammalian cells to visually assess ribozyme activity would hasten this translation. The future work will be to use this FACS compatible reporter system to screen libraries of *Tetrahymena* ribozyme mutants for structural mutations that would enhance the splicing activity of the ribozyme. Examination of the structure and activity relationship in these mutants would further provide insights into splicing by the *Tetrahymena* ribozyme and enable its applications as an efficient RNA repair agent.

The RNA targeting and modifying ability of the *Tetrahymena* trans-splicing ribozyme may be utilized as a potential RNA imaging agent. Ribozyme-mediated RNA detection *via* the use of the ribozyme-reporter system offers a novel strategy to non-invasively monitor changes in oncogene expression *in vivo*. Thus far techniques available to image gene expression in mice target exogenously transferred transgenes. This system would be the first step taken towards targeting over-expressed endogenous genes. Moreover detecting RNA levels *in vivo* could become particularly important in this era of RNA interference (RNAi). As RNAi moves towards clinical trials, validation of RNAi inhibition by imaging will offer a convenient way to evaluate the efficacy of RNA suppression.

## Acknowledgements

Work in the authors' laboratory is supported by the Burroughs Wellcome Fund, the Department of Defense Breast Cancer Research Program IDEA award (W81XWH-06-1-0251), and the National Cancer Institute ICMIC@Stanford (1P50CA114747). G.G. was grateful to the Stanford Cancer Biology Training Grant postdoctoral fellowship (PHS NRSA 5T32 CA09302-29).

## References

- 1 M. M. Waldrop, *Science*, 1989, **246**, 325.
- 2 T. R. Cech, *Annu. Rev. Biochem.*, 1990, **59**, 543.
- 3 T. Inoue, F. X. Sullivan and T. R. Cech, *Cell*, 1985, **43**, 431.
- 4 M. D. Been and T. R. Cech, *Cell*, 1987, **50**, 951.
- 5 B. A. Sullenger and T. R. Cech, *Nature*, 1994, **371**, 619.
- 6 J. T. Jones, S. W. Lee and B. A. Sullenger, *Nat. Med.*, 1996, **2**, 643.
- 7 N. Lan, R. P. Howrey, S. W. Lee, C. A. Smith and B. A. Sullenger, *Science*, 1998, **280**, 1593.
- 8 L. A. Phylactou, C. Darrah and M. J. Wood, *Nat. Genet.*, 1998, **18**, 378.
- 9 T. Watanabe and B. A. Sullenger, *Proc. Natl. Acad. Sci. U. S. A.*, 2000, **97**, 8490.
- 10 C. S. Rogers, C. G. Vanoye, B. A. Sullenger and A. L. George, Jr., *J. Clin. Invest.*, 2002, **110**, 1783.
- 11 K. J. Ryu, J. H. Kim and S. W. Lee, *Mol. Ther.*, 2003, **7**, 386.
- 12 B. G. Ayre, U. Kohler, H. M. Goodman and J. Haseloff, *Proc. Natl. Acad. Sci. U. S. A.*, 1999, **96**, 3507.
- 13 B. S. Kwon, H. S. Jung, M. S. Song, K. S. Cho, S. C. Kim, K. Kimm, J. S. Jeong, I. H. Kim and S. W. Lee, *Mol. Ther.*, 2005, **12**, 824.
- 14 M. Hagen and T. R. Cech, *EMBO J.*, 1999, **18**, 6491.
- 15 S. A. Woodson and T. R. Cech, *Biochemistry*, 1991, **30**, 2042.
- 16 R. B. Waring, J. A. Ray, S. W. Edwards, C. Scazzocchio and R. W. Davies, *Cell*, 1985, **40**, 371.
- 17 J. V. Price and T. R. Cech, *Science*, 1985, **228**, 719.
- 18 S. Hasegawa, W. C. Jackson, R. Y. Tsien and J. Rao, *Proc. Natl. Acad. Sci. U. S. A.*, 2003, **100**, 14892.
- 19 S. Hasegawa, J. W. Choi and J. Rao, *J. Am. Chem. Soc.*, 2004, **126**, 7158.
- 20 G. Zlokarnik, P. A. Negulescu, T. E. Knapp, L. Mere, N. Burres, L. Feng,

- M. Whitney, K. Roemer and R. Y. Tsien, *Science*, 1998, **279**, 84.
- 21 T. Wehrman, B. Kleaveland, J. H. Her, R. F. Balint and H. M. Blau, *Proc. Natl. Acad. Sci. U. S. A.*, 2002, **99**, 3469.
- 22 X. Yan and J. Rao, *unpublished data.*
- 23 S. Hasegawa, G. Gowrishankar and J. Rao, *ChemBiochem*, 2006, **7**, 925.
- 24 M.-K. So, G. Gowrishankar, S. Hasegawa and J. Rao, *submitted.*
- 25 T. F. Massoud and S. S. Gambhir, *Genes Dev.*, 2003, **17**, 545.
- 26 T. Wilson and J. W. Hastings, *Annu. Rev. Cell Dev. Biol.*, 1998, **14**, 197.
- 27 X. Fang, J. J. Li, J. Perlette, W. Tan and K. Wang, *Anal. Chem.*, 2000, **72**, 747A.
- 28 J. M. Levisky and R. H. Singer, *J. Cell Sci.*, 2003, **116**, 2833.
- 29 J. Perlette and W. Tan, *Anal. Chem.*, 2001, **73**, 5544.
- 30 A. Roivainen, T. Tolvanen, S. Salomaki, G. Lendvai, I. Velikyan, P. Numminen, M. Valila, H. Sipila, M. Bergstrom, P. Harkonen, H. Lonnberg and B. Langstrom, *J. Nucl. Med.*, 2004, **45**, 347.
- 31 S. Bhaumik, Z. Walls, M. Puttaraju, L. G. Mitchell and S. S. Gambhir, *Proc. Natl. Acad. Sci. U. S. A.*, 2004, **101**, 8693.
- 32 H. Chao, S. G. Mansfield, R. C. Bartel, S. Hiriyanna, L. G. Mitchell, M. A. Garcia-Blanco and C. E. Walsh, *Nat. Med.*, 2003, **9**, 1015.
- 33 X. Liu, Q. Jiang, S. G. Mansfield, M. Puttaraju, Y. Zhang, W. Zhou, J. A. Cohn, M. A. Garcia-Blanco, L. G. Mitchell and J. F. Engelhardt, *Nat. Biotechnol.*, 2002, **20**, 47.
- 34 M. Puttaraju, J. DiPasquale, C. C. Baker, L. G. Mitchell and M. A. Garcia-Blanco, *Mol. Ther.*, 2001, **4**, 105.
- 35 X. Zhuang, L. E. Bartley, H. P. Babcock, R. Russell, T. Ha, D. Herschlag and S. Chu, *Science*, 2000, **288**, 2048.
- 36 X. Zhuang, *Annu. Rev. Biophys. Biomol. Struct.*, 2005, **34**, 399.
- 37 Y. Shav-Tal, R. H. Singer and X. Darzacq, *Nat. Rev. Mol. Cell Biol.*, 2004, **5**, 855.
- 38 C. Molenaar, A. Abdule, A. Gena, H. J. Tanke and R. W. Dirks, *J. Cell Biol.*, 2004, **165**, 191.
- 39 J. C. Politz, R. A. Tuft, T. Pederson and R. H. Singer, *Curr. Biol.*, 1999, **9**, 285.
- 40 D. P. Bratu, B. J. Cha, M. M. Mhlanga, F. R. Kramer and S. Tyagi, *Proc. Natl. Acad. Sci. U. S. A.*, 2003, **100**, 13308.
- 41 E. Bertrand, P. Chartrand, M. Schaefer, S. M. Shenoy, R. H. Singer and R. M. Long, *Mol. Cell*, 1998, **2**, 437.
- 42 D. Fusco, N. Accornero, B. Lavoie, S. M. Shenoy, J. M. Blanchard, R. H. Singer and E. Bertrand, *Curr. Biol.*, 2003, **13**, 161.